

## Evaluation and inter-comparison of open road line source models currently in use in the Nordic countries

Janne Berger<sup>1)</sup>, Sam-Erik Walker<sup>1)</sup>, Bruce Denby<sup>1)</sup>, Ruwim Berkowicz<sup>2)</sup>,  
Per Løfstrøm<sup>2)</sup>, Matthias Ketzel<sup>2)</sup>, Jari Härkönen<sup>3)</sup>, Juha Nikmo<sup>3)</sup> and  
Ari Karppinen<sup>3)</sup>

<sup>1)</sup> Norwegian Institute for Air Research, P.O. Box 100, NO-2027 Kjeller, Norway

<sup>2)</sup> National Environmental Research Institute, P.O. Box 358, DK-4000 Roskilde, Denmark

<sup>3)</sup> Finnish Meteorological Institute, P.O. Box 503, FI-00101 Helsinki, Finland

Received 23 Dec. 2008, accepted 29 Apr. 2009 (Editor in charge of this article: Veli-Matti Kerminen)

Berger, J., Walker, S.-E., Denby, B., Berkowicz, R., Løfstrøm, P., Ketzel, M., Härkönen, J., Nikmo, J. & Karppinen, A. 2010: Evaluation and inter-comparison of open road line source models currently in use in the Nordic countries. *Boreal Env. Res.* 15: 319–334.

The aim of this study was to compare and evaluate operational open-road Gaussian line-source models currently in use in Norway, Denmark and Finland. Four models, HIWAY2-AQ, OML-Highway, CAR-FMI and WORM, were applied to datasets from three measurement campaigns from each of the mentioned countries. The results were assessed through analysis with regard to normalisation, wind speed, wind direction, horizontal profiles and stability. Generally, the correlation between model estimates and observations decreased when normalising with emissions, due to the significant positive correlation between observed concentrations and emissions. Furthermore, we found a reduction of bias when normalising the Norwegian and Danish data, caused by overestimation of the dispersion at lower emission values. Due to OML-Highway's more advanced parameterisation of traffic-produced turbulence, this model performed best at higher emission values when the influence of traffic density and vehicle speed on traffic produced turbulence was higher. With regard to horizontal profiles, the relative bias for CAR-FMI increased as a function of distance from the road, indicating that the Lagrangian time scales are too short.

### Introduction

Model comparison studies provide a robust basis for evaluation, development and improvement of models. When several models are applied to the same dataset, we obtain insight and knowledge on specific differences between the models, and on the parts of the models that perform well or poorly. Over the years, a number of operational open-road or highway dispersion models have been developed, e.g. the HIWAY models (1 to 4),

the CALINE models (1 to 4), GM and ROADWAY. A review of these models can be found in Sharma *et al.* (2004). Gaussian models, however, typically perform poorly under low wind-speed conditions, or when the wind direction is close to parallel to the road, as described in Benson (1992). In Oettl *et al.* (2001), the Gaussian line-source model CAR-FMI was compared with the Lagrangian dispersion model GRAL, with special emphasis on low wind-speed conditions. It was shown that CAR-FMI tended

to overestimate the  $\text{NO}_x$  concentrations, while GRAL underestimated them, which was mainly due to GRAL's special treatment of enhanced horizontal dispersion (meandering flows) under low winds. Similar comparison studies were performed by e.g. Levitin *et al.* (2005) where CAR-FMI and the Gaussian line-source model CALINE-4 were applied to a Finnish dataset. The results showed that both models performed better at a greater distance from the road, and poorest performance was seen for low winds and parallel wind directions.

In this study, we applied a modified version of the HIWAY-2 model called HIWAY2-AQ, the Danish OML-Highway model, the Finnish CAR-FMI model and the new Norwegian WORM model, to three datasets from Norway, Denmark and Finland, respectively. The study addressed only roadside environments at rural sites that were not influenced by any building obstacle; hence, we denote these environments rural and open. The comparison was aimed at analysing the variability and quality of these open-road line-source (ORLS) models. More specific aims were to (i) determine the traffic-related and meteorological conditions, for which further model development is needed, and (ii) to evaluate each model performance against datasets.

## Model descriptions

Four models were applied in this study. Three of these are operational at the institutions involved, while the WORM model is still under development at the Norwegian Institute of Air Research (NILU). Each model calculates concentrations at various receptor points by integrating concentrations from a set of infinitesimal point sources defined along each line-source using the Gaussian plume equation as a basis (Seinfeld and Pandis 1998):

$$C = \frac{Q}{u_h} \int_0^D f d\ell, \quad (1)$$

where  $C$  ( $\text{g m}^{-3}$ ) is the concentration at the receptor point,  $Q$  ( $\text{g m}^{-1} \text{s}^{-1}$ ) is the line source emission strength (assumed constant along the line source),  $u_h$  ( $\text{m s}^{-1}$ ) is the effective transport velocity,  $D$  (m) is the length of the line source,  $f$

( $\text{m}^{-2}$ ) is the plume dispersion function and  $\ell$  (m) is an arbitrary line. The function  $f$  is given as:

$$f = \frac{1}{2\pi\sigma_y\sigma_z} \exp\left(-\frac{y^2}{2\sigma_y^2}\right) \times \left[ \exp\left(-\frac{(z-h)^2}{2\sigma_z^2}\right) + \exp\left(-\frac{(z+h)^2}{2\sigma_z^2}\right) \right], \quad (2)$$

where  $\sigma_y$  and  $\sigma_z$  (m) are the Gaussian horizontal and vertical dispersion parameters, respectively,  $y$  and  $z$  (m) are coordinates and  $h$  (m) is the effective source height. The above formulation does not include internal reflections from the top of the boundary layer. Extra terms are included in some of the models to account for this. The effective transport velocity,  $u_h$ , transports the pollutants away from the source. Since the observed wind speeds in each dataset are measured at a higher level than  $h$ ,  $u_h$  must be calculated. Although each model uses different methods in order to calculate  $u_h$ , they all apply Monin-Obukhov similarity theory to extrapolate the measured wind speed down to the transport height:

$$u_h = u(z_1) \frac{\ln\left(\frac{h}{z_0}\right) - \psi_m\left(\frac{h}{L}\right) + \psi_m\left(\frac{z_0}{L}\right)}{\ln\left(\frac{z_1}{z_0}\right) - \psi_m\left(\frac{z_1}{L}\right) + \psi_m\left(\frac{z_0}{L}\right)}, \quad (3)$$

where  $u(z_1)$  ( $\text{m s}^{-1}$ ) is the measured wind speed at the measurement height  $z_1 > h$ ,  $z_0$  and  $L$  (m) are the surface roughness and Monin-Obukhov lengths, respectively, and  $\psi_m$  is the stability correction function (Businger *et al.* 1971). The explicit forms of this function can be found e.g. in Paulson (1970).

A common assumption in all the models is that the total Gaussian dispersion parameter,  $\sigma_{y,z}$ , can be represented as a combination of atmospheric turbulence,  $\sigma_{y,z,a}$ , and traffic-produced turbulence (TPT),  $\sigma_{y,z,t}$ , as

$$\sigma_{y,z}^2 = \sigma_{y,z,a}^2 + \sigma_{y,z,t}^2. \quad (4)$$

All models except form OML-Highway base their formulation of TPT on the formulation in the HIWAY-2 model (Petersen 1980), which is a semi-empirical treatment based on the General Motors experiments (Cadle *et al.* 1976):

$$\sigma_{z,\text{initial}} = 3.57 - 0.53U_c, \quad (5)$$

$$\sigma_{y,\text{initial}} = 2\sigma_{z,\text{initial}}. \quad (6)$$

Equations 5 and 6 represent the initial vertical and horizontal dispersions in the near vicinity of the source caused by turbulent mixing due to car wakes. The smallest allowable value of  $\sigma_{z,\text{initial}}$  is 1.5 m. The model includes a factor  $U_c$  called the aerodynamic drag, which accounts for the initial dilution of the pollutant on the roadway, and allows the model to make reasonable concentration estimates during low wind-speed conditions. An analysis of the General Motors data showed that  $U_c$  must depend on  $u_h$  and the horizontal angle of the wind to the roadway,  $\theta$  (deg):

$$U_c = 1.85u_h^{0.164} \cos^2 \theta. \quad (7)$$

Note that Eqs. 5 and 7 are numerical equations, and the units do not fit. For further details, see Petersen (1980).

### The HIWAY2-AQ model (NILU version of HIWAY-2)

The HIWAY2-AQ model is a modified version of the US EPA HIWAY-2 model (Petersen 1980), and is currently used as the operational sub-grid scale line source model in NILU's Air Quality Information and Management System (AirQUIS). It is a steady-state Gaussian model in which it is assumed that each lane of the highway is a continuous, finite line-source with a uniform emission rate.

In order to calculate downwind concentrations, three conditions are considered with regard to stability: in stable conditions, or if the mixing height  $h_{\text{mix}} > 5000$  m, Eq. 1 is used. In neutral or unstable conditions, if  $\sigma_z > 1.6h_{\text{mix}}$ , the distribution below the mixing height is uniform with height regardless of the source and receptor height, provided both are smaller than the mixing height. For all other unstable or neutral conditions multiple reflections from the mixing height and surface are also considered up to  $N$  reflections. However, due to the low level of the traffic sources and the close proximity of the measurements to the road, the mixing height did not play a significant role in the model calculations carried out in this study.

### Integration method

The trapezoidal rule together with the Richardson extrapolation is used to evaluate Eq. 1. This is based on the concept that a weighted average of two different estimates of the same value can be more accurate than either of the estimates, provided the weights are chosen appropriately to cancel the errors. The integration is iteratively solved for 9 iterations or until a predefined accuracy of 2% is achieved.

### Parameterisation of turbulence parameters

The HIWAY-2 model calculates the dispersion parameters,  $\sigma_y$  and  $\sigma_z$  using Pasquill-Gifford curves and stability classes (Turner 1969). However, in HIWAY2-AQ, only two stability conditions are used; classes A, B, C, representing unstable and D, representing neutral conditions, are all treated as neutral, i.e. class D, whilst classes E and F are both treated as lightly stable, i.e. class E. In Eq. 4,  $\sigma_{z_a}$  is of the form:

$$\sigma_{z_a} = ax^b, \quad (8)$$

where  $x$  (km) is the downwind distance from the source, and  $a$  and  $b$  are empirical factors depending on the atmospheric stability. On the other hand,  $\sigma_{y_a}$  is dependent on  $x$  and on the half angle of the horizontal spreading of the plume to the road,  $\theta_p$  (deg):

$$\sigma_{y_a} = \left( \frac{1000}{2.15} \right) x \tan \theta_p, \quad (9)$$

The value 2.15 is the number of standard deviations from the centreline of the Gaussian distribution to the point where the distribution falls to 10% of the centreline value.

TPT is modelled according to Eqs. 5–7.

### The OML-Highway model

The National Environmental Research Institute (NERI) in Denmark has developed the OML-Highway model. It is a local-scale Gaussian air pollution model based on boundary layer scaling, which estimates dispersion from point

sources and area sources. It comprises two versions; OML-Point 2.1, which is applicable to a single source, and OML-Multi 5.0, which allows multiple point and area sources. These underwent a revision in 2005–2006, but in this study we have used the Multi 5.0 version before the revision. OML-Highway has a meteorological pre-processor, which applies Monin-Obukhov similarity theory using synoptic, sonic and radiosonde data to calculate the required turbulent parameters.

### Integration method

OML-Highway treats the traffic lanes as area sources. It calculates the concentration at a receptor point by a double integral in the crosswind and the along-road wind directions. When the receptor is inside an area source, OML-Highway only integrates the upwind part of the area source. For crosswind directions it treats the road as a finite line source and applies the analytic solution of Eq. 1 with error functions similar to Eq. 11. However, for along-road wind directions, OML-Highway uses the Romberg integration technique (Press *et al.* 1992) with Richardson's extrapolation of the trapezoidal rule. At greater distances from the road, the numerical integration is replaced by a single line source for faster calculations. A more detailed description of the integration procedure can be found in Olesen *et al.* (2007).

### Calculation of effective dilution velocity, $u_h$

In order to estimate  $u_h$  for stable conditions, OML-Highway calculates an average wind speed between the ground and the emission height by integrating the wind profile (Eq. 3) between these heights. The minimum height at which the wind speed is calculated is  $z_{\min} = \max\{z, 10z_0\}$  (m). For unstable conditions, OML-Highway does not use average wind speeds but applies Eq. 3 to estimate the  $u_{h,\text{unstable}}$  at the emission height,  $h$ . In all conditions, a minimum wind speed given by  $u_{\min} = \max\{0.2, 0.6w^*\}$  m s<sup>-1</sup> is used, where  $w^*$  is the convective velocity scale ( $w^* = 0$  m s<sup>-1</sup> for neutral and stable conditions).

### Parameterisation of turbulence parameters

The parameterisation of  $\sigma_0$  is based on the formulation in the OSPM model (Berkowicz 2000), but is slightly modified with regard to highways in open environments, where traffic produced turbulent kinetic energy,  $e$  (m<sup>2</sup> s<sup>-2</sup>), is represented as a function of the number, the size and the speed of the vehicles. The assumption in OSPM of a constant TPT is not applicable to an open highway, as the concentrations are calculated at a greater distance from the road. It is therefore assumed that the velocity parameter, given as  $u_{\text{TPT}} = \sqrt{e}$  (m s<sup>-1</sup>) decays in an exponential manner with respect to distance from the source:

$$\sigma_0(t) = \sigma_{\text{initial}} + u_{\text{TPT}} \tau \left[ 1 - \exp\left(-\frac{t}{\tau}\right) \right], \quad (10)$$

where  $t$  is the transport time (s),  $\tau$  is the time scale for the decay of TPT (s) and  $\sigma_{\text{initial}} = 3.2$  m is the initial dispersion. These parameters have been determined empirically based on analysis of the Danish data used in this study.

### The CAR-FMI model

The CAR-FMI model (Contaminants in the Air from a Road) has been developed by the Finnish Meteorological Institute (FMI). It consists of an emission model, a dispersion model and a statistical analysis of the computed time-series of the concentrations. A more complete description of the model is presented in e.g. Härkönen *et al.* (1996). In this particular study, we applied the version that was used in the OSCAR (Optimised Expert System for Conducting Environmental Assessment of Urban Road Traffic) project. The meteorological pre-processor, MPP-FMI, is based on the method developed by van Ulden and Holtslag (1985). This method evaluates the turbulent heat and momentum fluxes in the atmospheric boundary layer (ABL) from observations. The parameterisation of the ABL height is based on the boundary layer scaling and meteorological sounding data (Karppinen *et al.* 1998), yielding hourly values of turbulence parameters, such as the Monin-Obukhov length scale, friction velocity and convective velocity scale, and boundary layer height.

## Integration method

The pollutant concentration is estimated from the analytical solution of Eq. 1, which is integrated over a finite line source in the lateral direction (Luhar and Patil 1989). Furthermore, the model assumes a total reflection from the ground, ignores reflection at the mixing height ( $h_{\text{mix}}$ ), and allows any wind direction with respect to the line source:

$$C = \frac{Q}{2\sqrt{2\pi}\sigma_z(u\sin\theta + u_0)} \times \left[ \exp\left(-\frac{(z-h)^2}{2\sigma_z^2}\right) + \exp\left(-\frac{(z+h)^2}{2\sigma_z^2}\right) \right] \times \left[ \operatorname{erf}\left(\frac{\sin\theta(p-y) - x\cos\theta}{\sqrt{2}\sigma_y}\right) + \operatorname{erf}\left(\frac{\sin\theta(p+y) + x\cos\theta}{\sqrt{2}\sigma_y}\right) \right], \quad (11)$$

where  $u$  ( $\text{m s}^{-1}$ ) is the average wind speed,  $u_0$  ( $\text{m s}^{-1}$ ) is a wind speed correction due to the turbulence induced by the traffic,  $x$ ,  $y$  and  $z$  (m) are the coordinates where the origin is at the centre of the line source,  $p$  (m) is the half length of the line source, erf is the error function and the other variables are as explained earlier. The numerical value of  $u_0 = 0.2 \text{ m s}^{-1}$  effectively removes the singularity when the wind direction is parallel to the road.

## Parameterisation of turbulence parameters

In MPP-FMI, the turbulence parameters are modelled as a function of the Monin-Obukhov length, friction velocity and mixing height. With regard to the atmospheric turbulence, the parameters are written in terms of turbulent intensities,  $i_{y,z}$  (Gryning *et al.* 1987):

$$\begin{aligned} \sigma_{y,z}^2 &= i_{y,z} f_{y,z} x, \\ i_{y,z} &= \frac{\sigma_{v,w}}{u(z)}, \\ f_{y,z} &= \left[ 1 + \sqrt{\frac{t}{2T_{L,y,z}}} \right]^{-1}, \end{aligned} \quad (12)$$

where  $f_{y,z}$  are functions of  $x$ ,  $\sigma_{v,w}$  ( $\text{m s}^{-1}$ ) are the standard deviations of the turbulence velocity fluctuations in the lateral and vertical directions,

$T_{L,y,z}$  (s) are the Lagrangian time scales and the other variables are as explained earlier.  $\sigma_v$  and  $\sigma_w$  are parameterised according to Gryning *et al.* (1987) and can be found in Härkönen *et al.* (1996).

With regard to TPT, the parameterisation is based on the same formulation as in the HIWAY-2 model (Eqs. 5–7).

## The WORM model

The WORM (Weak Wind Open Road Model) is currently under development at NILU (S. E. Walker unpubl. data). The version of the model applied in this study is quite similar to the CAR-FMI model, with some modifications regarding the integration technique and parameterisations used. The meteorological pre-processor is based on Monin-Obukhov similarity theory and equations for  $h_{\text{mix}}$  are applied as recommended by COST-710 (Fisher *et al.* 1998). The horizontal and vertical Lagrangian time scales ( $T_{L,y,z}$ ) were set to 300 s in this study.

## Integration method

WORM integrates the plume dispersion function over the line source using a highly accurate and efficient Gaussian quadrature method (Kythe and Schäferkötter 2005), which is accurate also for wind directions parallel to the road.

## Parameterisation of turbulence parameters

The horizontal and vertical turbulence profile used in this study are based on Gryning *et al.* (1987) with a minimum setting of  $\sigma_v$ ,  $\sigma_{v,\text{min}} = 0.5 \text{ m s}^{-1}$ , to reduce overestimated concentrations at low wind speeds. With regard to  $\sigma_y$ , WORM takes into account horizontal meandering for low wind speeds using an expression given in Oettl *et al.* (2005). The growth of  $\sigma_z$  currently uses the same formulation as in the CAR-FMI model (Eq. 12).

Regarding TPT, WORM currently uses the same formulation as the HIWAY-2 model (Eqs. 5–7). Table 1 summarizes the major features and differences between the models.

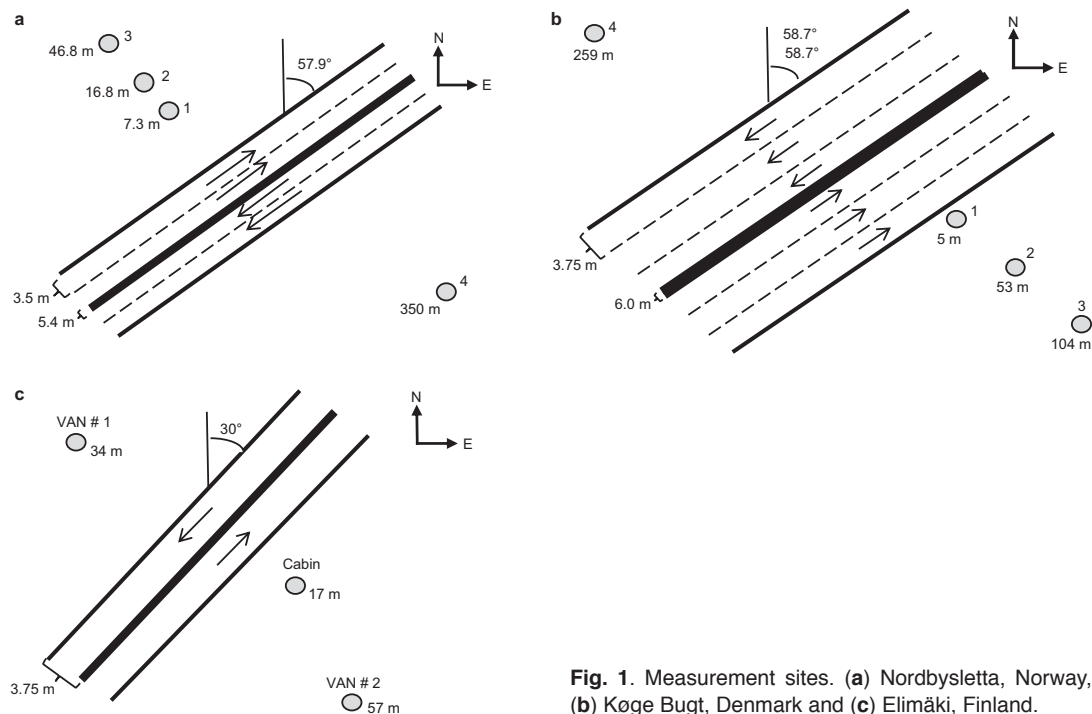


**Fig. 1.** Measurement sites. (a) Nordbysletta, Norway, (b) Køge Bugt, Denmark and (c) Elimäki, Finland.

## Measurement sites, datasets and emissions

The datasets consisted of air quality and meteorological measurements carried out near major roads/highways. Most of the campaigns included a number of stations placed at different distances from the road (Fig. 1, *see also* Table 2). The pollutant  $\text{NO}_x$  ( $\text{NO} + \text{NO}_2$ ) was considered, since this compound was measured at all sites, its emissions were best known and it could be treated as a tracer for the short time scales involved.

## Emissions

Emission inventories are calculated for each of the sites by the institutes responsible for the monitoring campaigns. However, in one case, Nordbysletta, the emissions were recalculated by the Danish institute, using the emission module WinOSPM.

The Norwegian emission dataset is calculated using the AirQUIS emission module. For line

sources, the module needs information such as traffic volume, speed, road characteristics (orientation, road width, etc.) and classification of vehicles. The emission factors are dependent on factors such as fuel, driving speed, slope and ageing factor (Denby *et al.* 2004) and are based on COPERT III (Ekström *et al.* 2004). According to this methodology, the  $\text{NO}_x$  emissions are set to zero when the traffic speed exceeds  $130 \text{ km h}^{-1}$ . In AirQUIS, however, this threshold is set to  $110 \text{ km h}^{-1}$ .

For the Danish data, the emissions are estimated based on traffic data from the Danish Public Roads Administration. These include number of vehicles and vehicle speed, with a classification into light and heavy duty vehicles. Based on these data the emission module in the Danish street pollution model OSPM, WinOSPM, calculates a time series of emissions (Jensen *et al.* 2004).

The emission model in CAR-FMI, which calculates vehicular CO and  $\text{NO}_x$ , is based on national emission factors of the traffic planning system KEHAR 2.0, developed by the Finnish Road Administration. Speed limit, type of road,



**Table 1.** Main features and differences between models.

	Norwegian Institute for Air Research	National Environmental Research Institute	Finnish Meteorological Institute	Norwegian Institute for Air Research
Model	HIWAY2-AQ	OML-Highway	CAR-FMI	WORM
Model type	Slender plume Gaussian steady state	Slender plume Gaussian steady state	Slender plume Gaussian steady state	Slender plume Gaussian steady state
Met. data	Single height wind speed, direction, mixing layer. Pasquill-Gifford stability class	Different options, either sonic data or radiosonde	MPP-FMI boundary layer scaling	Single height wind and temperature profiles
Calculation of $u_h$	Monin-Obukhov similarity theory ( $\psi_m = 0$ , $h = 2$ m)	Monin-Obukhov similarity theory (different for stable and unstable conditions)	Monin-Obukhov similarity theory ( $h = 2$ m)	Monin-Obukhov similarity theory ( $h = 2$ m)
$u_{min}$ (m s <sup>-1</sup> )	–	max{0.2, 0.6 $w^*$ }	0.2	0.5
Stability described using	Pasquill-Gifford stability classes	Monin-Obukhov similarity theory	Monin-Obukhov similarity theory	Monin-Obukhov similarity theory
$h_{mix}$	Boundary layer parameter based on $u^*$	Pre-processor or from measurements	MPP-FMI	COST-710 eq.
$T_L$	–	Implicit, dependent on met. conditions	Unstable, $L < 0$ : $T_L = 300$ sec, stable, $L > 0$ : $T_L = 30$ sec	$T_L = 300$ sec
Integration method	Numerical, Richardson extrapolation	Analytical for crosswind direction, numerical for along wind direction	Analytical (Luhar and Patil 1989)	Numerical, Gaussian quadrature
TPT	Semi-empirical (Petersen 1980)	Empirical, exponential decay of TPT with distance from source	Semi-empirical (Petersen 1980)	Semi-empirical (Petersen 1980)

traffic flow, the share of heavy duty vehicles and the year for the computations is used as input.

Methodology

In this study, the four models were applied to the three datasets and analysed statistically. The overall model performance on all data were assessed using the Pearson coefficient of determination (denoted by  $R^2$ ) and relative bias (denoted by RB), where

$$R^2 = \frac{\left[ n(\sum C_{pred} C_{obs}) - \sum C_{pred} \sum C_{obs} \right]^2}{\left\{ n(\sum C_{pred}^2) - (\sum C_{pred})^2 \right\} \left\{ n(\sum C_{obs}^2) - (\sum C_{obs})^2 \right\}}, \quad (13)$$

where  $n$  is the number of data points,  $C_{pred}$  is the predicted concentration ( $\text{g m}^{-3}$ ) and  $C_{obs}$  is the observed concentrations ( $\text{g m}^{-3}$ ), and

$$RB = (C_{pred} - C_{obs})/C_{obs}. \quad (14)$$

Handling and selection of the datasets

Since in this study we were interested in the comparison of the models we concentrated largely on

the dispersion parts of the models. Several methodologies were at our disposal to do this:

- Model performance were assessed after dividing both observed and model-calculated concentrations by emissions  $Q$  ( $Q$ -normalisation).
- The ratios of modelled/observed concentrations for different meteorological conditions were compared.
- Model performance as a function of a distance from the road were assessed using  $Q$ -normalised concentrations.
- Model performance with regard to atmospheric stability were assessed using the  $Q$ -normalised concentrations.

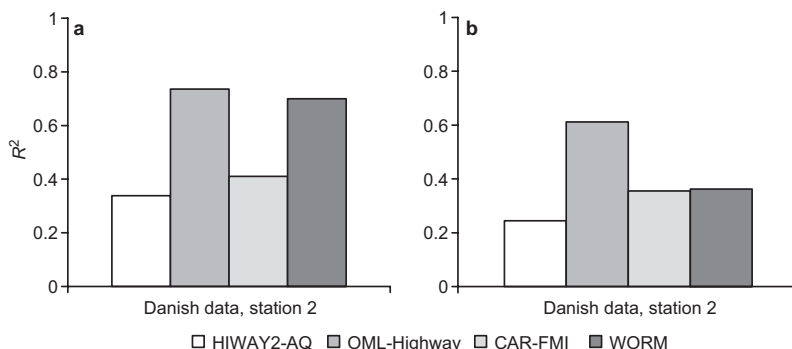
Note that in some cases, we present results only from stations 3 and 2 from the Norwegian and Danish dataset, respectively, as these stations were located at similar distances from the road (Fig. 1). With regard to the Finnish site, the station VAN #1 was the only station where the air quality measurement height was 3.5 m, i.e. a similar measurement height as for the stations at the Norwegian and Danish sites (*see* Table 2); hence, this station was used in the analysis. Furthermore, due to time constraints OML-Highway was not

Table 2. Site and measurement characteristics.

Site	Nordbysletta, Norway	Køge Bugt, Denmark	Elimäki, Finland
Time of campaign	1 Jan.–15 Apr. 2002	17 Sep.–18 Dec. 2003	15 Sep–30 Oct. 1995
Number of datapoints	~900	~900	~75
Number of stations (background excluded)	3	3	1
Length of road segment (m)	~850	1485	~2000
Number of lanes	4	6	2
Orientation of road (due north)	57.9°	58.7°	30°
Traffic flow (veh. day <sup>-1</sup> )	~36000	~100000	~7200
Speed limit (km h <sup>-1</sup> )	90	110	100
Meteorological measurements	Cup anemometer: hourly wind speed, wind direction, temperature, vertical temperature difference between 10 m and 2 m, global solar radiation	Ultrasonic anemometer: hourly wind speed, temperature, etc. Rural background site: hourly global solar radiation data	Hourly wind speed, temperature, wind direction, global solar radiation, relative humidity
Height of meteorological measurements (m)	10	8	3.5, 6 and 10
Height of air quality measurements (m)	3.5	3	3.5
Roughness length (m)	0.25	~0.1	0.2
Average wind speed (m s <sup>-1</sup> )	~2.3	~4.5	~3



**Fig. 2.** Coefficient of determination ( $R^2$ ) for all models applied to the Danish data (station 2): (a) non-normalised results, (b)  $Q$ -normalised results.



applied to the Finnish data. Finally, in all cases we subtracted the background concentration from the measurements and compared these net observed concentrations with the model predictions.

### Uncertainties in input data

Regarding emission data, accurate traffic counts were available from all sites so these data should be of relatively good quality. However, when the traffic is low, a large “statistical” uncertainty occurs. Although low emission values do not play a large role in the absolute concentrations, they are quite important when normalising with emissions. Therefore, we used a minimum value of 300 vehicles per hour as a lower limit for the  $Q$ -normalised data.

There is a high relative uncertainty in the wind speed measurements when the wind speeds are low ( $< 1 \text{ m s}^{-1}$ ). In addition, for low wind speeds, the mean wind direction is not well defined. This is particularly important for wind directions parallel to the road.

## Results and discussion

### Concentrations normalised with emissions

The main feature for all models is a decrease of  $R^2$  in case of normalized data, due to the natural positive correlation between observations and emissions (Table 3 and Fig. 2). Scatter plots of modelled *versus* observed  $\text{NO}_x$  for OML-Highway and WORM applied to the Norwe-

gian and Danish data, respectively, are shown in Fig. 3. Generally, when  $Q$ -normalising the concentrations, the larger the decrease in  $R^2$ , in respect to the non-normalised values, then fewer dispersion parameters are related to the observations. Another feature is a decrease in RB when normalising; this is particularly evident for WORM applied to the Danish data (Fig. 3). As mentioned, the Danish institute recalculated the Norwegian emissions. This was found to result in a difference of  $\sim 0.1$  in the RB, and did not affect  $R^2$ . RB for all models applied to the Norwegian, Danish and Finnish data (Fig. 4) shows that it is evident that the values of RB for the models applied to the Finnish data were similar for both non-normalised and  $Q$ -normalised concentrations (Table 4). However, in the Danish dataset, and also to a lesser extent in the Norwegian dataset, RBs of the  $Q$ -normalised concentrations were smaller than RBs of the non-normalised concentrations. This was true for the majority of the models. An analysis of the  $Q$ -normalised modelled and observed concentrations *versus* emissions (not shown here), showed that the majority of the models underestimated the observed concentrations when the emissions, and hence the traffic volumes, were low, and overestimated when the emissions were high. Therefore, a decrease of RB occurred when normalising the concentrations with the emissions, since the concentrations were underestimated at low emissions (low traffic volumes). Assuming the emissions are valid, though less certain for lesser traffic volumes, this indicated that all the models overestimated the dispersion at lower traffic volumes and this in turn was related to the initial dispersion by TPT. In all models, an

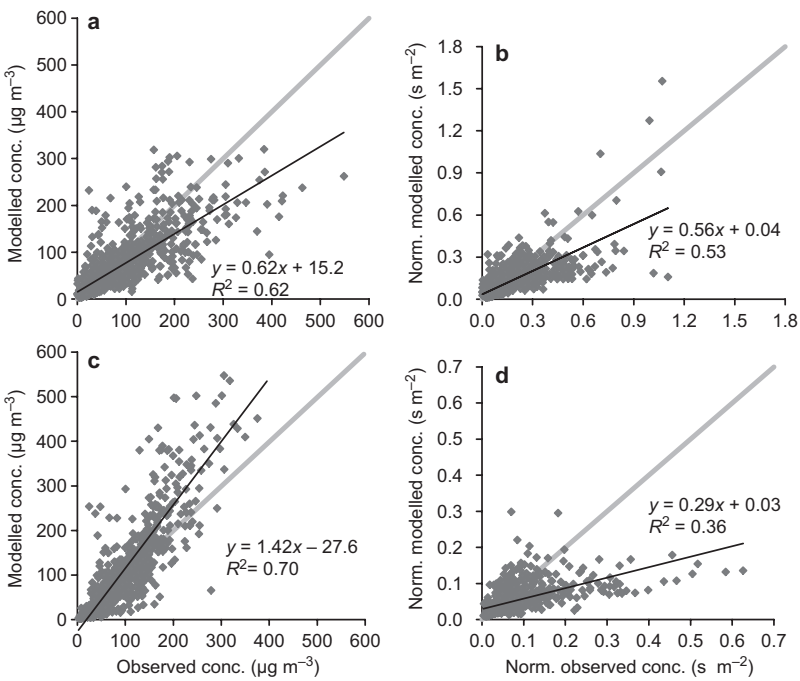


**Fig. 3.** Scatter plots of modelled *versus* observed concentrations, for (a) OML: Norwegian data (station 3) non-normalised, (b) OML: Norwegian data (station 3) *Q*-normalised, (c) WORM: Danish data (station 2) non-normalised, (d) WORM: Danish data (station 2) *Q*-normalised. Included in the plots are the one-to-one line (grey line) and the linear regression fit (black line), with the regression model and coefficient of determination ( $R^2$ ).

**Table 3.** Coefficient of determination,  $R^2$  for all models applied to all data, for both non-normalised and *Q*-normalised results.

	HIWAY2-AQ Non-norm.	HIWAY2-AQ <i>Q</i> -norm.	OML-Highway Non-norm.	OML-Highway <i>Q</i> -norm.	CAR-FMI Non-norm.	CAR-FMI <i>Q</i> -norm.	WORM Non-norm.	WORM <i>Q</i> -norm.
Norwegian data								
St. 1	0.50	0.18	0.72	0.69	0.50	0.23	0.72	0.42
St. 2	0.52	0.21	0.68	0.60	0.46	0.28	0.68	0.47
St. 3	0.48	0.20	0.62	0.53	0.46	0.37	0.64	0.49
Danish data								
St. 1	0.38	0.18	0.75	0.65	0.49	0.25	0.65	0.28
St. 2	0.34	0.24	0.74	0.61	0.41	0.36	0.70	0.36
St. 3	0.31	0.27	0.71	0.56	0.43	0.50	0.71	0.43
Finnish data								
VAN#1	0.51	0.49	—	—	0.47	0.44	0.51	0.51

**Table 4.** Relative bias, RB, for all models applied to all data, for both non-normalised and *Q*-normalised results.

	HIWAY2-AQ Non-norm.	HIWAY2-AQ <i>Q</i> -norm.	OML-Highway Non-norm.	OML-Highway <i>Q</i> -norm.	CAR-FMI Non-norm.	CAR-FMI <i>Q</i> -norm.	WORM Non-norm.	WORM <i>Q</i> -norm.
Norwegian data								
St. 1	0.02	−0.16	−0.21	−0.22	−0.11	−0.16	−0.31	−0.34
St. 2	0.13	−0.07	−0.19	−0.19	0.03	−0.02	−0.26	−0.29
St. 3	0.12	−0.10	−0.20	−0.22	0.18	0.12	−0.24	−0.28
Danish data								
St. 1	0.16	−0.27	0.04	−0.18	0.42	0.08	0.11	−0.22
St. 2	0.15	−0.35	0.00	−0.30	0.67	0.24	0.13	−0.26
St. 3	0.06	−0.42	0.01	−0.31	0.74	0.29	0.10	−0.28
Finnish data								
VAN#1	−0.13	−0.14	—	—	0.09	0.09	−0.48	−0.49

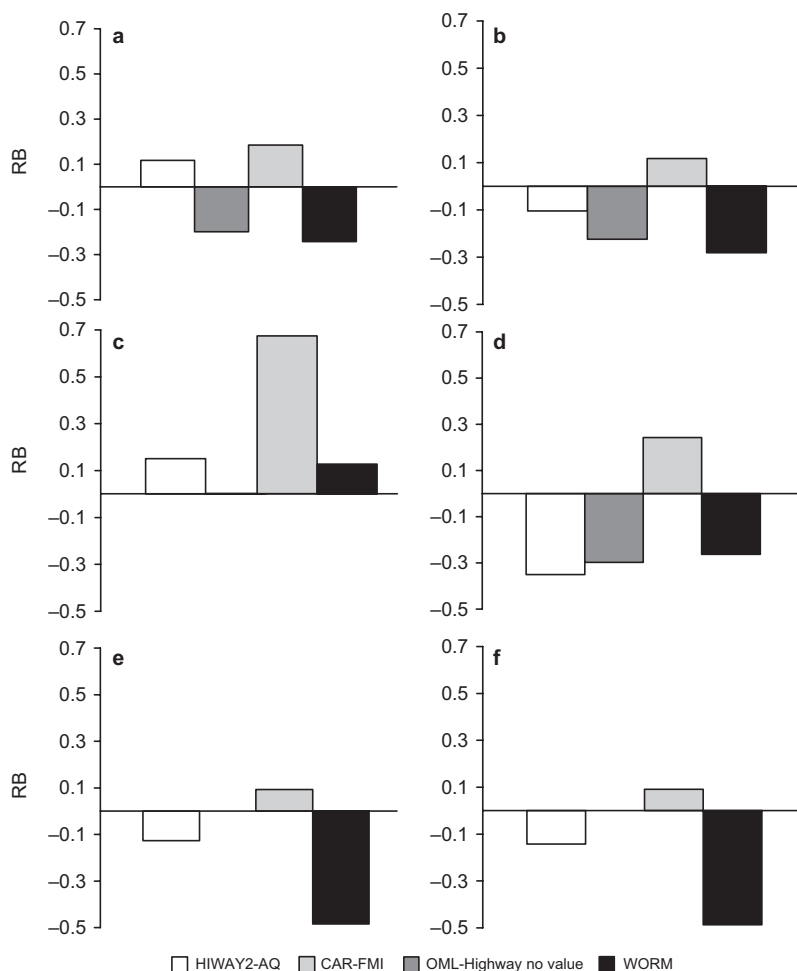


**Fig. 4.** Relative bias (RB) for all models applied to the Norwegian (station 3), Danish (station 2) and Finnish (VAN station) data. (a) Norwegian (station 3) non-normalised, (b) Norwegian (station 3) Q-normalised, (c) Danish (station 2) non-normalised, (d) Danish (station 2) Q-normalised, (e) Finnish (VAN station) non-normalised, (f) Finnish (VAN station) Q-normalised.

initial dispersion  $\sigma_{z,initial}$  (Eqs. 5 and 10) was used and this appeared to be too large for low traffic volumes, by roughly a factor of three.

With regard to overestimation at higher emission values, analysis (not shown here) also showed that all models except OML-Highway overestimated more for high emission values when applied to the Danish data than when applied to the Norwegian data. This causes the different behaviour with regard to OML-Highway and WORM applied to the Norwegian and Danish data (Fig. 3), respectively. The Danish measurements were carried out on a highway with much higher traffic than the Norwegian ones; ~100 000 vehicles per day as compared with ~36 000 vehicles per day, respectively. The average vehicle speed at the Danish site was also higher, ~109 km h<sup>-1</sup> as compared with ~90 km h<sup>-1</sup>

at the Norwegian site. As a result, dilution due to TPT should be higher at this site. OML-Highway performed better for higher emissions due to its formulation of TPT, based on parameterisation of the decay of turbulent kinetic energy. Below, we discuss this feature in more detail with regard to wind speed.

### The effect of wind speed and wind direction

Scatter plots of the ratio of modelled to observed concentrations *versus* wind speed at 2 m above ground for all models applied to the Norwegian and Danish data at stations 3 and 2, respectively (Fig. 5), show that more scatter and over-predictions were present for low wind-speed condi-

tions, due to more uncertainty in the modelling and the observations; the latter will lead to scatter irrespective of the quality of the modelling. For the Norwegian data at higher wind speeds, underestimations were evident, more so than on the Danish site. This difference occurred as a result of the differences between the datasets with regard to traffic volumes as previously mentioned; higher traffic volumes and emissions at the Danish site imply greater significance of TPT, and the TPT formulation in HIWAY2-AQ, CAR-FMI and WORM was not adequate in this respect.

The ratio of modelled to observed concentrations *versus* wind direction for all models applied to the Norwegian and Danish data (Fig. 6), show that the largest scatter, with significant overestimate, was present under wind directions parallel to the road. Some models performed poorly under such conditions due to inaccuracies in the integration methods, in particular the analytical Luhar and Patil approximation as used by CAR-FMI, but also to a certain extent the trapezoidal method with Richardson extrapolation as used by HIWAY2-AQ. However, observational uncertainties also played a role, as wind directions parallel to the road were poorly defined, especially for low wind speeds. WORM proved to perform best in this regard, although not perfect, as the overestimations are slightly reduced. WORM is also the only model applying Gaussian quadrature as a numerical integration technique, which is highly accurate even for parallel wind directions.

## Horizontal profiles

In order to study how the models perform with regard to distance from the road, it was useful to study the  $Q$ -normalised RB for each station at the Norwegian and Danish sites (Fig. 7). The behaviour of RB is dependent on the initial dispersion,  $\sigma_{z, \text{initial}}$ , caused by TPT, and the atmospheric dispersion. When applied to both datasets, RB for CAR-FMI increased with increasing distance from the road, indicating that the dispersion did not evolve at the rate indicated by the observations. The Lagrangian time scales,  $T_L$ , were probably too small in this model (under

stable conditions,  $T_L = 30$  sec, *see* Table 1). For both datasets, stable and unstable conditions amounted to  $\sim 40\%$  and  $15\%$ – $20\%$  of the total amount of hours, respectively. Hence, short time scales dominated, and the overestimate became more pronounced with time and distance from the source. This is shown in Eq. 12 where short time scales imply less dispersion. With regard to all models except CAR-FMI and to a lesser extent WORM, the values of RB decreased as a function of distance from the source, when applied to the Danish data. The average observed wind speed at the Danish site was higher than at the Norwegian site ( $4.6 \text{ m s}^{-1}$  and  $2.6 \text{ m s}^{-1}$ , respectively). Hence, the atmospheric turbulence played a more significant role as the significance of TPT decreases with distance from the source.

## The effect of stability

Differences between the datasets appear clearly when studying RB for all models applied to the Danish and Norwegian datasets for different Pasquill-Gifford stability classes (Turner 1969) for the  $Q$ -normalised concentrations (Fig. 8). With regard to the Norwegian data, the majority of the models underestimated the concentrations for all stability classes. However, a larger degree of overestimate, especially for unstable conditions, was evident when the Danish dataset is applied, consistent with the analysis in 5.1 and 5.2. HIWAY2-AQ, on the other hand, consistently overestimated the unstable conditions on both datasets because it uses the neutral class for all unstable cases, hence, it did not describe all of the dispersion, which clearly is a weakness with the model. CAR-FMI stood out with regard to its consistent overestimate of stable conditions (classes E–F). For CAR-FMI, this indicated that the positive biases (Figs. 4 and 7) were caused by the stable conditions, which represented most of the data. For both datasets, the lowest observed wind speeds occurred under unstable and stable conditions (classes A–C and E–F, respectively), while the highest observed wind speeds occurred under neutral conditions (class D), where the biases were closest to zero (especially at the Danish site), hence, this was consistent with the distribution of bias discussed earlier

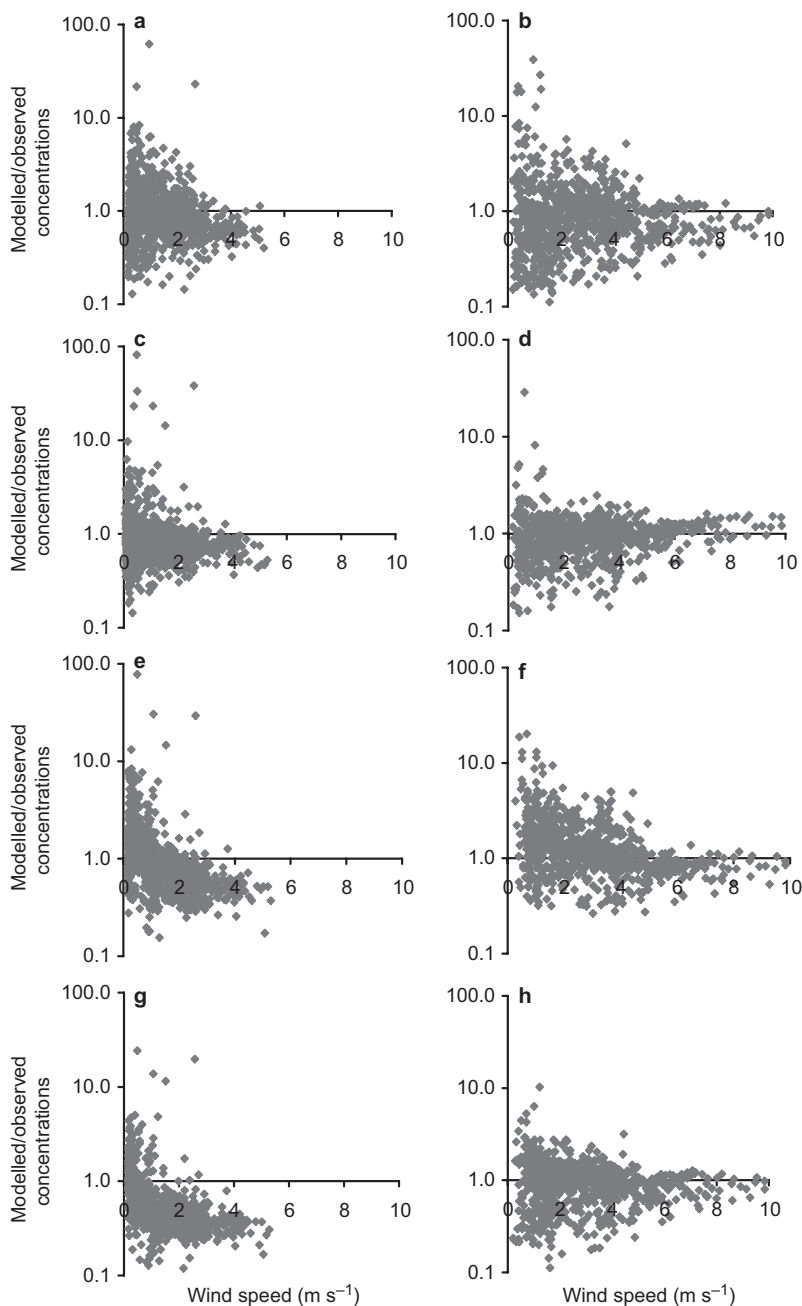


**Fig. 5.** Scatter plots of the ratio of modelled to observed concentrations *versus* wind speed at 2 m above ground for all models applied to the Norwegian (**a, c, e, g**: station 3) and Danish (**b, d, f, h**: station 2) data.

(Fig. 5). For all stability classes, OML-Highway performed best with regard to bias because of its formulation of TPT. It was therefore likely that OML-Highway's formulation of TPT also played a significant role in model performance with regard to stability; however, as mentioned, the initial  $\sigma_{z,initial}$  must be revised.

## Conclusions

Four open road line source models were compared and evaluated based on their application on datasets from measurement campaigns in Norway, Denmark and Finland. The specific aim was to determine under which conditions the

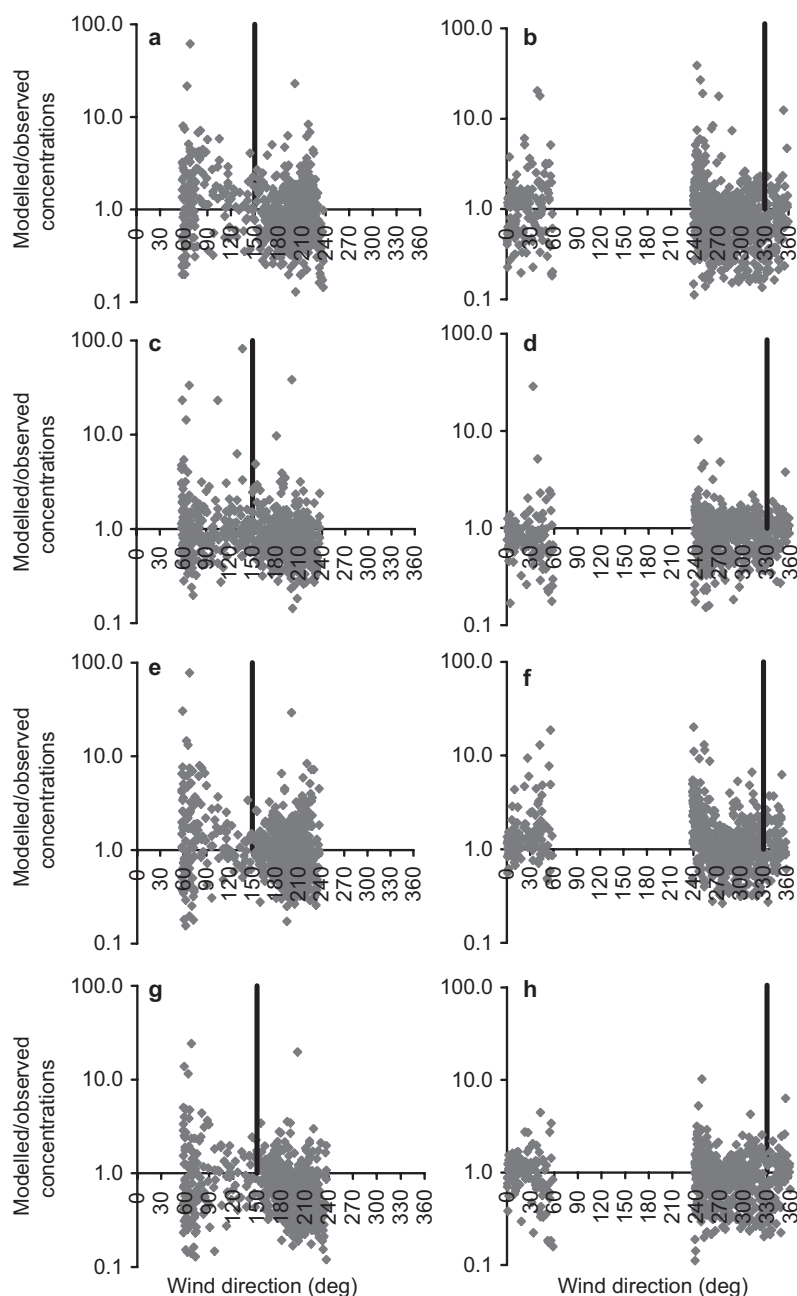


**Fig. 6.** Same as Fig. 5, but plotted against wind direction with respect to north. The vertical lines indicate the direction perpendicular to the road when the stations are downwind of the road.

models perform well or poorly. The measurement campaigns were conducted near highways in open environments.

When normalising with emissions,  $R^2$  generally decreased as the natural positive correlation between emissions and observations is removed. Analysis of the data indicated that reduction in RB in the Norwegian and Danish data after

normalising was caused by overestimation of the dispersion at lower traffic volumes and lower emission values. This occurred because the initial dispersion,  $\sigma_{z,initial}$ , was too large in all the models. Also, all models except OML-Highway gave higher RB for high emission values when applied to the Danish data than when applied to the Norwegian data, due to the increased sig-

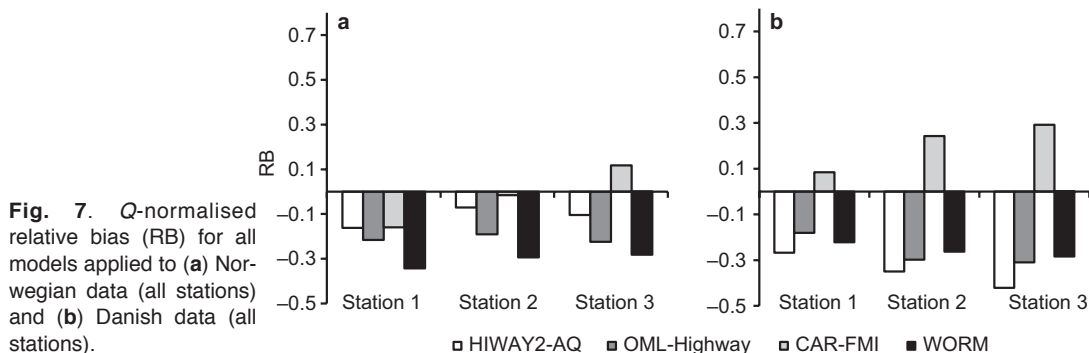


**Fig. 7.** Q-normalised relative bias (RB) for all models applied to (a) Norwegian data (all stations) and (b) Danish data (all stations).

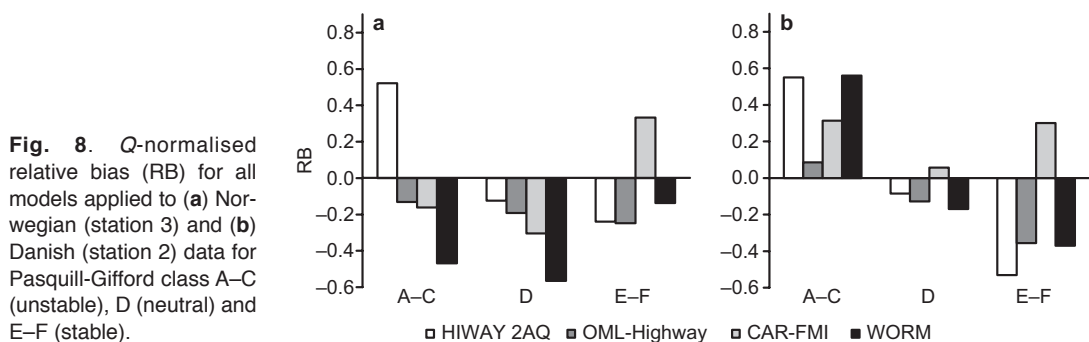


**Fig. 8.** Q-normalised relative bias (RB) for all models applied to (a) Norwegian (station 3) and (b) Danish (station 2) data for Pasquill-Gifford class A-C (unstable), D (neutral) and E-F (stable).

nificance of TPT at the more heavily trafficked Danish site. The latter feature was also seen in the scatter plots of the ratio of modelled to observed concentrations *versus* wind speed, at higher wind speeds. OML-Highway performed best in this regard due to its parameterisation of TPT based on decay of turbulent kinetic energy.

OML-Highway's parameterisation of TPT (or similar ones), should be implemented in ORLS models, to describe the turbulence produced by the traffic. However, the initial dispersion must be reduced in order to describe the concentrations when the emissions are low. The OML-Highway formulation is currently being implemented in WORM. Furthermore, in order to reduce uncertainties appearing under near to parallel wind directions, Gaussian quadrature methods, or other highly accurate numerical integration methods, should be implemented in ORLS models.

With regard to horizontal profiles, RB for CAR-FMI increased with increasing distance from the road. This indicates that the Lagrangian time scales,  $T_L$ , are too short, and need to be revised. RB for the other models decreased with distance from road at the Danish site, which is

an indication of the increased significance of atmospheric turbulence at larger distances from the road.

It is important that the effective transport velocity,  $u_h$ , and the height at which it is calculated is well described and documented, as  $u_h$  is highly important for the dispersion of pollutants. The stability corrections [e.g. the Businger-Dyer relations (Businger *et al.* 1971)] should be included.

*Acknowledgements:* Authors would like to thank John S. Irwin for his useful comments.

## References

- Benson P. 1992. A review of the development and application of the CALINE3 and 4 models. *Atmos. Environ.* 26B: 379–390.
- Businger J.A., Wyngaard J.C., Izumi Y. & Bradley E.F. 1971. Flux-profile relationships in the atmospheric surface layer. *J. Atmos. Sci.* 28: 181–189.
- Berkowicz R. 2000. OSPM — parameterised street pollution model. *Environmental Monitoring and Assessment* 65: 323–331.
- Cadle S.H., Chock D.P., Heuss J.M. & Monson P.R. 1976.



- Results of general motors sulfate dispersion experiments.* Report GMR-2107, General Motors Research Labs., Warren, MI.
- Denby, B., Laupsa, H. & McInnes, H. 2004. *AirQUIS2003. Models module — user's guide.* NILU TR 5/2004.
- Ekström M., Sjödin Å. & Andreasson K. 2004. Evaluation of the COPERT III emission model with on-road optical remote sensing measurements. *Atmos. Environ.* 38: 6631–6641.
- Fisher B.E.A., Erbrink J.J., Finardi S., Jeannot P., Joffre S., Morselli M.G., Pechinger U., Seibert P. & Thomson D.J. 1998. *COST Action 710 — Final report. Harmonisation of the pre-processing of meteorological data for atmospheric dispersion models.* EUR 18195. Luxembourg: Office for Official Publications of the European Communities.
- Gryning S.E., Jensen N.O. & Troen I. 1987. Turbulence and diffusion over inhomogeneous terrain. *Bound.-Layer Meteor.* 41: 173–202.
- Härkönen J., Valkonen E., Kukkonen J., Rantakrans E., Lahtinen K., Karppinen A. & Jalkanen L. 1996. *A model for the dispersion of pollution from a road network.* Publications on Air Quality 23, Finnish Meteorological Institute, Helsinki.
- Jensen S.S., Løfstrøm P., Berkowicz R., Olesen H.R., Frydendall J., Fuglsang K. & Hummelshøj P. 2004. *Luftkvalitet langs motorveje. Målekampagne og modelberegninger.* NERI Technical Report no. 522.
- Karppinen A., Kukkonen J., Nordlund G., Rantakrans E. & Valkama I. 1998. *A dispersion modelling system for urban air pollution.* Publications on Air Quality 28, Finnish Meteorological Institute, Helsinki.
- Kythe P.K. & Schäferkotter M.R. 2005. *Handbook of computational methods for integration.* Chapman & Hall/CRC, Boca Raton, FL.
- Levitin J., Härkönen J., Kukkonen J. & Nikmo J. 2005. Evaluation of the CALINE 4 and CAR-FMI models against measurements near a major road. *Atmos. Environ.* 39: 4439–4452.
- Luhar A. & Patil R. 1989. A general finite line source model for vehicular pollution dispersion. *Atmos. Environ.* 23: 555–562.
- Oettl D., Kukkonen J., Almbauer R.A., Sturm P.J., Pohjola M. & Härkönen J. 2001. Evaluation of a Gaussian and a Lagrangian model against a roadside data set, with emphasis on low wind speed conditions. *Atmos. Environ.* 35: 2123–2132.
- Oettl D., Goulart A., Degrazia G. & Anfossi D. 2005. A new hypothesis on meandering atmospheric flows in low wind speed conditions. *Atmos. Environ.* 39: 1739–1748.
- Olesen H.R., Berkowicz R. & Løfstrøm P. 2007. *OML-highway: review of model formulation.* NERI Technical Report no. 609.
- Paulson C.A. 1970. The mathematical representation of wind and temperature profiles in the unstable atmospheric surface layer. *J. Appl. Meteor.* 9: 857–861.
- Petersen W.B. 1980. *User's guide for HIWAY-2. A highway air pollution model.* EPA-600/8-80-018, U.S. EPA, Research Triangle Park, NC.
- Press W.H., Flannery B.P., Teukolsky S.A. & Vetterling W.T. 1992. *Numerical recipes in FORTRAN: The art of scientific computing*, 2nd ed. Cambridge University Press, Cambridge.
- Seinfeld J.H. & Pandis S.N. 1998. *Atmospheric chemistry and physics. From air pollution to climate change.* John Wiley & Sons, New York.
- Sharma N., Chaudry K.K. & Chalapati Rao C.V. 2004. Vehicular pollution prediction modelling: a review of highway dispersion models. *Transport Reviews* 24: 409–435.
- Turner D.B. 1969. *Workbook of atmospheric dispersion estimates.* Public Health Service Publication no. 999-AP-26, U.S. Public Health Service, Cincinnati, OH.
- van Ulden A.P. & Holtslag A.A.M. 1985. Estimation of atmospheric boundary layer parameters for diffusion applications. *J. Clim. Appl. Meteorol.* 24: 1196–1207.